

000 HARNESSING UNCERTAINTY: ENTROPY-MODULATED 001 POLICY GRADIENTS FOR LONG-HORIZON LLM 002 AGENTS 003

004
005
006 **Anonymous authors**
007 Paper under double-blind review
008
009
010
011
012

ABSTRACT

013 In long-horizon tasks, recent agents based on Large Language Models (LLMs)
014 face a significant challenge that sparse, outcome-based rewards make it difficult
015 to assign credit to intermediate steps. Previous methods mainly focus on creating
016 dense reward signals to guide learning, either through traditional reinforcement
017 learning techniques like reward shaping and intrinsic motivation or by using Process
018 Reward Models for step-by-step feedback. In this paper, we identify a fundamental
019 problem in the learning dynamics of LLMs: the magnitude of policy gradients is
020 inherently coupled with the entropy, which leads to inefficient small updates for
021 confident correct actions and potentially destabilizes large updates for uncertain
022 ones. To resolve this, we propose Entropy-Modulated Policy Gradients (EMPG),
023 a framework that re-calibrates the learning signal based on step-wise uncertainty
024 and the final task outcome. EMPG amplifies updates for confident correct actions,
025 penalizes confident errors, and attenuates updates from uncertain steps to stabilize
026 exploration. We further introduce a bonus term for future clarity that encourages
027 agents to find more predictable solution paths. Through comprehensive experiments
028 on three challenging agent tasks, WebShop, ALFWorld, and Deep Search, we
029 demonstrate that EMPG achieves substantial performance gains and significantly
030 outperforms strong policy gradient baselines.
031
032

1 INTRODUCTION

033 The advent of Large Language Models (LLMs) has catalyzed the development of autonomous agents
034 that are capable of tackling complex, multi-step tasks (Wei et al., 2022; Yao et al., 2023). However,
035 a fundamental challenge persists in training these agents for long-horizon tasks: the sparsity of
036 outcome-based rewards. In many realistic scenarios, such as web navigation (Yao et al., 2022),
037 software engineering Zhang et al. (2024), and deep search (Alzubi et al., 2025), feedback is only
038 available at the end of the complete generation. This makes it difficult to assign appropriate credit for
039 standard reinforcement learning (RL) algorithms to discern the crucial intermediate steps.
040

041 To address sparse rewards, prior work has explored either densifying reward signals via techniques
042 like reward shaping and intrinsic motivation, or providing explicit step-wise supervision with Process
043 Reward Models (PRMs) (Lightman et al., 2023). Both approaches face significant hurdles. Reward
044 densification methods often fail to scale to the vast state-action spaces of LLM agents, while PRMs
045 are prohibitively expensive to annotate, struggle with generalization, and are impractical for complex
046 interactive tasks where defining a single "correct" intermediate step is often impossible.
047

048 Policy entropy has also been repurposed as a learning signal. Some methods use entropy minimization
049 as an unsupervised objective to increase model certainty (Gao et al., 2025; Agarwal et al., 2025), but
050 risk inducing "hallucinated confidence" where the model becomes confidently incorrect Zhang et al.
051 (2025d). More recent work uses entropy to modulate the learning signal in single-turn, reasoning
052 tasks (Chen et al., 2025; Cheng et al., 2025). However, it remains underexplored how to leverage an
053 agent's intrinsic uncertainty for credit assignment in long-horizon, multi-step decision-making.
054

055 Our work begins by analyzing the fundamental dynamics of the policy gradient itself. We formally
056 show that for a standard softmax policy, the expected norm of the score function is a monotonic
057 function of the policy's entropy (Proposition 1). In simple terms, high-entropy (uncertain) actions
058

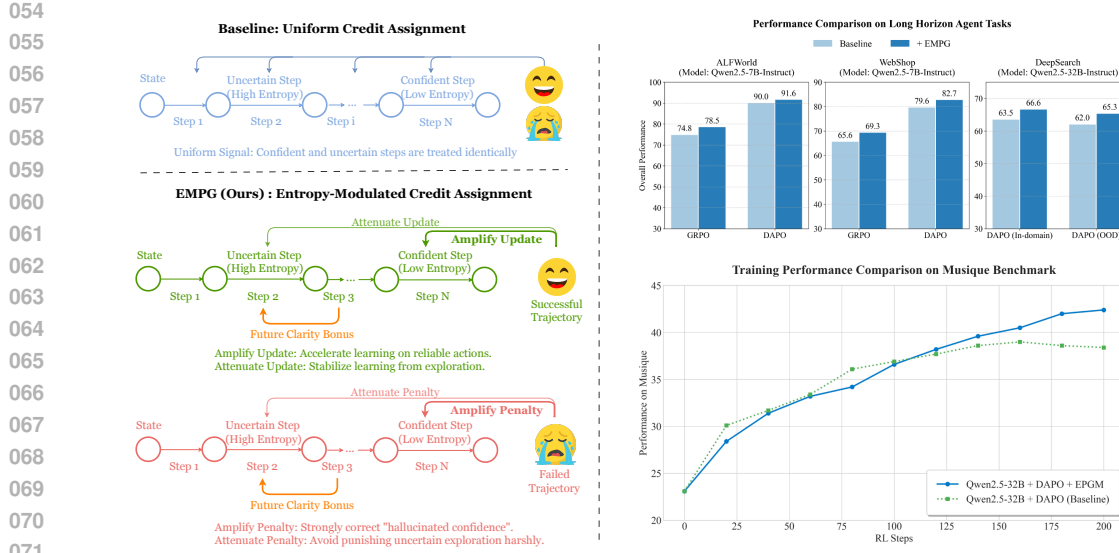


Figure 1: Overview of the EMPG mechanism and its algorithm performance. **Left:** Conceptual diagram contrasting the uniform credit assignment of baseline methods with EMPG’s confidence-modulated signal. **Right:** Final performance comparison on key long-horizon benchmarks showing EMPG’s superiority, along with the training dynamics on Musique that highlight its ability to achieve sustained improvement and avoid the baseline’s performance plateau.

naturally produce large gradients, while low-entropy (confident) actions produce small ones. This inherent behavior presents a dual challenge for learning: 1) confident and correct steps, which should be strongly reinforced, receive small updates, limiting learning speed, and 2) uncertain exploratory steps can introduce large, noisy gradients that destabilize training. This reveals a critical need to explicitly re-calibrate the learning signal based on an action’s uncertainty.

To address this, we propose Entropy-Modulated Policy Gradients (EMPG), a framework that reshapes the learning landscape by directly adapting to this dynamic, as illustrated in Figure 1. Instead of naively rewarding low entropy, EMPG introduces *Self-Calibrating Gradient Scaling* mechanism, which dynamically modulates the policy gradient based on step-wise uncertainty: 1) *for confident and correct actions*, it amplifies the updates, while 2) *for uncertain steps*, it attenuates updates to ensure stable exploration. Furthermore, to encourage agents to find predictable solution paths, EMPG introduces “*future clarity*”, an additional bonus term in the advantage function that provides an intrinsic signal for actions that lead to less uncertain subsequent states. This guides agents to perform purposeful exploration, steering them away from chaotic or unpromising high-entropy trajectories toward states with greater clarity about the next steps. This dual approach enables EMPG to forge a dense, informative, and well-calibrated learning signal from sparse external feedback. To validate our framework, we conduct experiments on challenging long-horizon agent benchmarks such as WebShop Yao et al. (2022), ALFWorld Shridhar et al. (2021), and Deep Search Alzubi et al. (2025), demonstrating the effectiveness and scalability of our approach across models of various sizes.

Our key contributions are as follows:

- We first identify and formalize a fundamental challenge in policy gradient methods: the inherent coupling of gradient magnitude and policy entropy. This dynamic leads to inefficient learning for confident actions and instability from uncertain ones, motivating the need for explicit signal re-calibration.
- We introduce Entropy-Modulated Policy Gradients, a framework designed to solve this problem. EMPG combines *Self-Calibrating Gradient Scaling* to correct the flawed gradient dynamics with a *Future Clarity Bonus* to promote exploration towards more predictable states.
- Extensive experiments on demanding agent tasks (WebShop, ALFWorld, Deep Search) show that EMPG substantially outperforms strong baselines like GRPO and DAPO.

108

2 RELATED WORK

109

110 2.1 LLM-BASED AUTONOMOUS AGENTS

111 The advent of LLMs has catalyzed the development of sophisticated autonomous agents capable of
 112 performing complex, multi-step tasks that were previously unattainable. Specialized agents have
 113 been designed for diverse applications, including software development (e.g., coding agents (Zhang
 114 et al., 2024)), information retrieval (search agents (He et al., 2025; Li et al., 2025)), and complex web
 115 interactions (browser-use agents (Yao et al., 2022; Deng et al., 2023; Yan et al., 2023)). For training
 116 these agentic models, reinforcement learning has proven to be a powerful and essential paradigm.
 117 Recent research on RL-based agents, such as Search-R1 (Jin et al., 2025), SWE-RL (Wei et al.,
 118 2025a), and WebAgent-R1 (Wei et al., 2025b), has demonstrated that RL can effectively enhance
 119 agent performance and enable learning in highly interactive and dynamic environments. Despite these
 120 successes, a fundamental problem remains to be fully addressed: the difficulty of credit assignment
 121 in long-horizon tasks. The multi-step nature of these problems, where a reward signal is often only
 122 available upon completion, hinders the efficiency and stability of the training process.
 123

124

125 2.2 REINFORCEMENT LEARNING FROM INTERNAL FEEDBACK

126 To overcome the challenges of sparse external rewards, recent studies have explored using internal
 127 feedback, generated by the model itself, to create denser training signals. This approach often
 128 leverages unsupervised signals derived from model uncertainty (Zhang et al., 2025b; Agarwal et al.,
 129 2025; Zhao et al., 2025) or self-consistency (Zuo et al., 2025; Zhang et al., 2025a), frequently
 130 quantified by policy entropy. However, the role of entropy has been interpreted in conflicting
 131 ways. Some studies argue that correct responses typically exhibit lower entropy, thus proposing
 132 unsupervised entropy minimization as a method to improve performance (Gao et al., 2025); for
 133 example, Agarwal et al. (2025) focuses on minimizing the entropy of the entire generated trajectory
 134 to enhance the confidence and quality of the final output, typically in single-turn reasoning tasks.
 135 Conversely, other works suggest that high entropy encourages exploratory reasoning. For instance,
 136 SEED-GRPO (Chen et al., 2025) uses semantic entropy to modulate policy updates for diversity,
 137 while others explicitly incorporate policy entropy into the advantage term to promote exploration
 138 (Cheng et al., 2025; Vanlioglu, 2025). Recently, EDGE-GRPO (Zhang et al., 2025c) proposes entropy
 139 modulation in single-turn mathematical reasoning. Similar to our method, they modulate policy
 140 gradients by amplifying updates for confident correct responses and attenuating updates for incorrect
 141 or uncertain ones. However, EMPG fundamentally differs from EDGE-GRPO in both motivation and
 142 scope: First, while EDGE-GRPO focuses on correcting confidence misalignment within a single-turn
 143 mathematical reasoning, EMPG is specifically designed for the multi-step credit assignment problem
 144 in long-horizon tasks. Second, towards the challenges in multi-turn long-horizon tasks, EMPG
 145 dynamically assigns credit across the entire trajectory to amplify the crucial steps.
 146

147

148 3 PRELIMINARIES

149

150 3.1 BACKGROUND: POLICY OPTIMIZATION FOR LONG-HORIZON AGENT TASKS

151 We formalize the long-horizon agent task as a reinforcement learning problem where an LLM-based
 152 policy, π_θ , is optimized to maximize the expected total return, $R(\tau)$. A foundational approach in this
 153 domain is Proximal Policy Optimization (PPO), which ensures training stability by using a learned
 154 value model to estimate step-wise advantages (Schulman et al., 2017). However, this approach
 155 introduces substantial memory and computational overhead. Furthermore, its effectiveness hinges on
 156 value estimates that are difficult to learn accurately, especially in sparse-reward, long-horizon tasks.
 157

158 Due to these challenges, value-free policy gradient methods have become a popular and effective
 159 paradigm, as they avoid the overhead and instability of a learned value function (Shao et al., 2024;
 160 Yu et al., 2025). Methods like Group Relative Policy Optimization (GRPO) and Decoupled Clip and
 161 Dynamic Sampling Policy Optimization (DAPO) provide robust credit assignment by comparing
 162 multiple trajectory rollouts. While effective at avoiding value model pitfalls, these strategies still rely
 163 on coarse, trajectory-level credit assignment. This fails to pinpoint critical actions and ignores the
 164 rich, intrinsic signal of the model’s own step-wise uncertainty—the very signal our work leverages.
 165 Details are provided in Appendix B.

162 3.2 THEORETICAL MOTIVATION: A TWO-PART RE-CALIBRATION OF POLICY GRADIENTS
163

164 Our approach is motivated by a fundamental analysis of the relationship between a policy’s gradient
165 and its predictive uncertainty. Standard policy gradients, while effective, possess an inherent dynamic
166 that can hinder stable and efficient learning. Specifically, the magnitude of the gradient is inherently
167 coupled with the policy’s entropy, often leading to inefficiently small updates for confident actions and
168 potentially destabilizing large updates for uncertain ones. This dynamic, which we aim to re-calibrate,
169 is formally characterized by the following proposition.

170 **Proposition 1.** *For a policy π_θ parameterized by a softmax over logits $z_\theta(s)$, the expected squared
171 L2-norm of the score function $\nabla_{z_\theta} \log \pi_\theta(a|s)$ with respect to the logits is a direct function of the
172 policy’s Rényi-2 entropy Rényi (1961), $H_2(\pi)$:*

$$173 \mathbb{E}_{a \sim \pi_\theta(\cdot|s)} [||\nabla_{z_\theta(s)} \log \pi_\theta(a|s)||^2] = 1 - \exp(-H_2(\pi_\theta(\cdot|s))) \quad (1)$$

175 A detailed proof is provided in Appendix C.

177 Equation 1, which builds upon established relationships between different measures of policy entropy
178 (e.g., in Li (2025)), proves that the expected gradient norm is monotonically coupled with policy
179 entropy. This presents a dual challenge: 1) a confident and correct step should be reinforced strongly,
180 but its naturally small gradient limits its impact; and 2) the large gradients from highly uncertain
181 exploratory steps can introduce noise and destabilize training. Our first component, *Self-Calibrating*
182 *Gradient Scaling*, directly addresses this by re-calibrating the *magnitude* of the update based on
183 current-step uncertainty.

184 However, re-calibrating the update magnitude is only half the solution. A truly effective learning
185 signal must also guide the agent in a useful *direction*. This motivates our second component, the
186 *Future Clarity Bonus*, which can be conceptually justified through the lens of information theory.
187 **The Future Clarity Bonus is formulated as a step-wise intrinsic reward that encourages the agent
188 to select actions a_t that lead to low-entropy (high clarity) subsequent states s_{t+1} .** By rewarding the
189 immediate clarity gained, the bonus encourages actions that yield high *Information Gain* about the
190 optimal future path. Crucially, this is a local, step-wise objective aimed at minimizing the policy’s
191 entropy *at the next state*, rather than minimizing the entropy of the full trajectory:

$$192 \min_{a_t} H(\pi_\theta(\cdot|s_{t+1})). \quad (2)$$

194 This objective, which aligns with established principles like the Empowerment framework Klyubin
195 et al. (2005), imbues the agent with a generalizable meta-skill: to actively seek clarity in the face of
196 ambiguity, effectively turning the complex problem at s_t into a “more solvable” or “less ambiguous”
197 sub-problem at s_{t+1} .

198 In summary, EMPG provides a complete, two-part re-calibration of the learning signal. The gradient
199 scaling module ensures each update has an appropriate *magnitude*, while the future clarity bonus
200 provides a principled intrinsic motivation that shapes the policy’s *direction* towards robust and
201 predictable solution paths.

203 4 ENTROPY-MODULATED POLICY GRADIENTS
204

205 Building on the theoretical motivation established in our preliminaries, we introduce Entropy-
206 Modulated Policy Gradients (EMPG), a framework designed to re-calibrate the learning dynamics of
207 policy gradients for long-horizon agent tasks. As shown in Section 3.2, standard policy gradients
208 are inherently biased towards applying smaller updates to confident (low-entropy) steps and larger
209 updates to uncertain (high-entropy) ones. EMPG is engineered to counteract this behavior, enabling
210 more efficient and stable learning from sparse, outcome-based rewards.

212 4.1 QUANTIFYING STEP-LEVEL UNCERTAINTY
213

214 The core of our method is to quantify the agent’s confidence at each decision-making step. While
215 various uncertainty measures exist, we opt for a practical and computationally efficient proxy: the
average token-level entropy over a single “reason-then-act” step. For a step $step_t$ composed of tokens

216 $\{w_1, \dots, w_m\}$, the step-level entropy H_t is:
 217

$$218 \quad 219 \quad 220 \quad H_t = -\frac{1}{m} \sum_{j=1}^m \sum_{v \in V} p(v|w_{<j}) \log p(v|w_{<j}) \quad (3)$$

221 where $p(v|w_{<j})$ is the probability of token v from the vocabulary V , as provided by the LLM’s policy
 222 π_θ . A lower H_t indicates higher confidence in the generated step, corresponding to a lower-entropy
 223 state in the sense of Proposition 1. **This Shannon entropy formulation is utilized as a robust and**
 224 **efficient proxy because, for any distribution, it is monotonically related to the Rényi-2 entropy**
 225 **($H(\pi) \geq H_2(\pi)$), thus tracking the same core uncertainty principle.**

226 While we use policy entropy for its computational efficiency, future work could explore alternative
 227 uncertainty estimators, such as those derived from Monte Carlo dropout or the variance in logits
 228 from an ensemble of model heads. However, we believe entropy provides the most direct link to the
 229 gradient dynamics analyzed in Proposition 1, making it the most theoretically grounded choice for
 230 our framework.

232 4.2 THE MODULATED ADVANTAGE FOR GRADIENT RE-CALIBRATING

234 In the sparse reward setting, a standard RL advantage function provides a uniform learning signal for
 235 all steps within a single trajectory. While simple, this approach overlooks the varying contributions of
 236 different steps and their impact on learning stability. To address this, we introduce a novel, modulated
 237 advantage estimate, A_{mod} , for each step t in a trajectory τ_i :

$$238 \quad 239 \quad 240 \quad A_{\text{mod}}(i, t) = \underbrace{A^{(i)} \cdot g(H_t^{(i)})}_{\text{self-calibrating gradient scaling}} + \underbrace{\zeta \cdot f(H_{t+1}^{(i)})}_{\text{future clarity bonus}} \quad (4)$$

242 This formulation fundamentally re-calibrates the learning signal through two complementary forms of
 243 **advantage shaping**. The first term utilizes a step-level entropy-based function $g(H_t^{(i)})$ to dynamically
 244 reweight the trajectory’s shared advantage $A^{(i)}$, thereby achieving a more granular and confidence-
 245 aware gradient update. The second term, a **future clarity bonus**, is an additive shaping signal that
 246 encourages the agent to select actions that lead to a more predictable and less ambiguous future state.
 247 Together, these two mechanisms transform a coarse, trajectory-level signal into a rich and precise
 248 learning signal for each step, which we analyze further in the following sections.

249 **Self-Calibrating Gradient Scaling $g(H)$.** To counteract the natural gradient dynamics, the scaling
 250 function $g(H)$ is designed to be self-calibrating and adaptive. It achieves this by enforcing the
 251 constraint that the mean of $g(H_t^{(i)})$ over any given mini-batch is normalized to one. Mathematically,
 252 for a mini-batch of size N_B , this constraint is given by:

$$255 \quad 256 \quad 257 \quad \frac{1}{\sum_{i=1}^{N_B} T_i} \sum_{i=1}^{N_B} \sum_{t=1}^{T_i} g(H_t^{(i)}) = 1 \quad (5)$$

258 This principled design ensures the modulation redistributes the learning signal rather than simply
 259 inflating or deflating it, offering stability, adaptivity, and a reduction in hyperparameters. We
 260 implement this by normalizing a base exponential function by its mean over the mini-batch:

$$261 \quad 262 \quad 263 \quad 264 \quad g(H_t^{(i)}) = \frac{\exp(-k \cdot H_{\text{norm}, t}^{(i)})}{\sum_{j=1}^{N_B} \sum_{t'=1}^{T_j} \exp(-k \cdot H_{\text{norm}, t'}^{(i)})} \quad (6)$$

265 For a confident step ($H_t^{(i)}$ is lower than the batch average), $g(H_t^{(i)}) > 1$, which **amplifies** its gradient.
 266 This accelerates convergence for confident and correct decisions ($A^{(i)} > 0$) and provides a strong
 267 corrective penalty for confident errors ($A^{(i)} < 0$), combating “hallucinated confidence”. Conversely,
 268 for an uncertain step ($H_t^{(i)}$ is higher than average), $g(H_t^{(i)}) < 1$, which **attenuates** its gradient,
 269 preventing noisy updates from high-entropy exploration from destabilizing the policy.

270 **Algorithm 1** Entropy-Modulated Policy Gradients (EMPG)

```

271 1: Initialize: Policy  $\pi_\theta$ .
272 2: for each training iteration do
273 3:   Collect a batch of trajectories  $\mathcal{B} = \{\tau_i\}$  by running policy  $\pi_\theta$ .
274 4:   Calculate outcome-based advantages  $A^{(i)}$  for each trajectory  $\tau_i \in \mathcal{B}$ .
275 5:   Compute all step-level entropies  $\{H_t\}$  for all steps in the batch.
276 6:   Normalize all entropies  $\{H_t\}$  to  $\{H_{\text{norm},t}\}$  using batch min-max scaling.
277 7:   Compute the self-calibrating scaling factors  $\{g(H_t)\}$  for all steps using Eq. 6.
278 8:   for each step  $t$  in each trajectory  $\tau_i$  do
279 9:     Calculate future clarity bonus  $f(H_{t+1}^{(i)})$  using Eq. 7.
280 10:    Compute modulated advantage  $A_{\text{mod}}(i, t)$  using Eq. 4.
281 11:   end for
282 12:   Normalize the batch of all modulated advantages to get  $\{A_{\text{final}}(i, t)\}$ .
283 13:   Update policy parameters  $\theta$  using policy gradients with  $\{A_{\text{final}}(i, t)\}$ .
284 14: end for
285

```

286 **Future Clarity Bonus $f(H)$.** Beyond re-calibrating individual step updates, EMPG also encourages
 287 the agent to find globally stable and predictable solution paths. The second term in Eq. 4 serves as an
 288 intrinsic motivation for this goal:

$$289 \quad f(H_{t+1}^{(i)}) = \exp(-k' \cdot H_{\text{norm},t+1}^{(i)}) \quad (7)$$

290 This term adds a positive bonus proportional to the confidence (low entropy) of the **next** step.
 291 Weighted by the hyperparameter $\zeta > 0$, this "future clarity" bonus actively guides the agent away
 292 from states of high confusion and towards sequences of high-quality, unambiguous decisions.

293 4.3 NORMALIZATION PROCEDURES

294 **Batch-Level Entropy Normalization.** To ensure the modulation function $g(H)$ operates on a
 295 consistent scale, we normalize step-level entropies within each training batch using min-max scaling.
 296 This stateless approach allows the normalization to adapt dynamically to the policy's evolving
 297 confidence level. For each entropy value H_t in the batch:

$$301 \quad H_{\text{norm},t}^{(i)} = \frac{H_t^{(i)} - \min_{\text{batch}}(H)}{\max_{\text{batch}}(H) - \min_{\text{batch}}(H) + \epsilon} \quad (8)$$

302 **Final Advantage Normalization.** After computing the modulated advantage A_{mod} for all steps in a
 303 batch, we perform a final batch-level normalization (zero mean). This standard variance reduction
 304 technique, which is crucial for stable policy updates, is achieved by subtracting the mean of A_{mod}
 305 over the mini-batch of size N_B :

$$306 \quad A_{\text{final}}(i, t) = A_{\text{mod}}(i, t) - \frac{1}{N_B} \sum_{j=1}^{N_B} \sum_{t_j=1}^{T_j} A_{\text{mod}}(j, t_j) \quad (9)$$

307 The overall EMPG algorithm is summarized in Algorithm 1, with an implementation provided in the
 308 appendix H. Furthermore, we provide a rigorous theoretical derivation for the EMPG update rule in
 309 Appendix D.

310 5 EXPERIMENTS

311 5.1 EXPERIMENTAL SETUP

312 **Tasks and Benchmarks.** We evaluate our method on three challenging long-horizon agent bench-
 313 marks featuring sparse, binary success rewards: WebShop (Yao et al., 2022), a web navigation task
 314 requiring complex instruction following; ALFWorld (Shridhar et al., 2021), a text-based environment
 315 combining instruction following with common-sense reasoning; and Deep Search Jin et al. (2025),
 316 a multi-step information retrieval and synthesis task. For Deep Search, we further categorize the
 317 evaluation sets into in-domain (ID) and out-of-domain (OOD) to assess generalization.

324 **Models and Agent Framework.** Our agent employs the ReAct paradigm (Yao et al., 2023), where
 325 the LLM first generates a thought before producing an action. For WebShop and ALFWorld, we use
 326 Qwen2.5-1.5B-Instruct (Yang et al., 2024) and Qwen2.5-7B-Instruct to compare our results with
 327 existing work. For the more complex Deep Search task, we use the powerful Qwen2.5-32B-Instruct
 328 model to conduct in-depth analysis.

329 **Baselines and Implementation.** We compare EMPG against strong policy gradient baselines:
 330 GRPO (Shao et al., 2024) and DAPO (Yu et al., 2025). Our method, EMPG, is implemented as
 331 an advantage modulation module that is applied directly on top of these baselines. This allows
 332 us to fairly measure the benefits of leveraging intrinsic uncertainty signals. For the WebShop and
 333 ALFWorld benchmarks, we based our implementation on the public codebase of GiGPO (Feng et al.,
 334 2025) for a fair comparison. For the DeepSearch benchmark, we curated a training dataset of 17k
 335 instances by filtering from several sources, including WebWalker (Wu et al., 2025), HotpotQA (Yang
 336 et al., 2018), 2WikiMultiHopQA (Ho et al., 2020), NaturalQuestions (Kwiatkowski et al., 2019), and
 337 TriviaQA (Joshi et al., 2017).

339 5.2 MAIN RESULTS

341 Our comprehensive experiments demonstrate that EMPG yields significant and consistent perfor-
 342 mance improvements across a diverse range of tasks, baselines, and model scales.

344 **Performance on ALFWorld and WebShop.** As shown in Table 1, EMPG serves as a robust
 345 enhancement to existing policy optimization algorithms. On the Qwen2.5-1.5B model, applying
 346 EMPG boosts the average success rate of GRPO on ALFWorld by +8.1 points and DAPO by +7.3
 347 points. This effectiveness scales to the larger Qwen2.5-7B model, where EMPG again improves both
 348 baselines on ALFWorld and elevates the DAPO success rate on WebShop to 82.7%. These results
 349 confirm that EMPG is highly compatible and provides reliable gains for different RL backbones.

351 **Performance and Scalability on Deep Search.** To investigate the scalability of our approach
 352 on more powerful models and complex retrieval tasks, we evaluated EMPG on the Deep Search
 353 benchmark using the Qwen2.5-32B-Instruct model. The results, presented in Table 2, further validate
 354 our method. Applying EMPG to the strong DAPO baseline boosts the overall average score from
 355 62.0 to 65.3, a substantial improvement of +3.3 points. This performance gain is notably robust,
 356 with EMPG improving the in-domain average by +3.1 points and demonstrating even stronger
 357 generalization with a +3.9 point gain on out-of-domain tasks.

358 Taken together, the results across all three benchmarks confirm that EMPG is a versatile and scalable
 359 enhancement for training LLM agents. It consistently improves performance regardless of the
 360 underlying RL algorithm, the nature of the task, or the size of the base model, validating our core
 361 hypothesis that leveraging intrinsic uncertainty is a powerful tool for learning from sparse rewards.

362 5.3 ANALYSIS

364 To understand the mechanisms behind EMPG’s effectiveness, we conduct a series of in-depth
 365 analyses focusing on three key questions: (1) What are the individual contributions of EMPG’s core
 366 components? (2) How does EMPG affect the learning process over time? (3) Why is a step-level
 367 analysis of entropy crucial?

369 **Ablation Study and Generalization Analysis.** To dissect the contributions of our method’s two
 370 main components, we perform a detailed ablation study using the results from the Deep Search
 371 benchmark, as presented in Table 2. The study reveals a distinct and complementary duality in
 372 their roles, which stems from how they shape the policy during training. The *Future Clarity Bonus*
 373 acts as a powerful *exploitation* signal during training. By reinforcing known, high-quality decision
 374 sequences within the training data, it helps the model master the in-domain distribution, leading to
 375 a strong performance gain of +2.6 points on ID tasks. Conversely, the *Self-Calibrating Gradient*
 376 *Scaling* serves as a powerful *regularization* mechanism during training, teaching the model how
 377 to behave when it is uncertain. By attenuating updates for high-entropy steps, it produces a final
 378 policy that is inherently more robust and less brittle. This learned robustness is then observed during

378 Table 1: Performance on ALFWorld and WebShop. Results are averaged over 3 random seeds. For
 379 ALFWorld, we report the average success rate (%) for each subtask as well as the overall result. For
 380 WebShop, we report both the average score and the average success rate (%). Methods marked with *
 381 are our reproduced results. The remaining results are adopted from GiGPO Feng et al. (2025).

Method	ALFWorld							WebShop	
	Pick	Look	Clean	Heat	Cool	Pick2	All	Score	Succ.
<i>Base: Closed-Source Model</i>									
Prompting GPT-4o	75.3	60.8	31.2	56.7	21.6	49.8	48.0	31.8	23.7
Prompting Gemini-2.5-Pro	92.8	63.3	62.1	69.0	26.6	58.7	60.3	42.5	35.9
<i>Base: Qwen2.5-1.5B-Instruct</i>									
Prompting Qwen2.5	5.9	5.5	3.3	9.7	4.2	0.0	4.1	23.1	5.2
Prompting ReAct	17.4	20.5	15.7	6.2	7.7	2.0	12.8	40.1	11.3
Prompting Reflexion	35.3	22.2	21.7	13.6	19.4	3.7	21.8	55.8	21.9
RL Training PPO (with critic)	64.8	40.5	57.1	60.6	46.4	47.4	54.4	73.8	51.5
RL Training RLOO	88.3	52.8	71.0	62.8	66.4	56.9	69.7	73.9	52.1
RL Training GRPO*	87.9 ± 6.3	40.0 ± 5.8	78.1 ± 3.8	35.7 ± 4.3	65.2 ± 1.2	44.4 ± 1.4	65.6 ± 2.9	78.0 ± 1.1	58.2 ± 2.4
with EMPG*	85.5 ± 4.8	33.5 ± 6.4	78.9 ± 2.5	76.2 ± 9.7	74.7 ± 1.9	69.1 ± 6.4	73.7 ± 2.7 (+8.1)	80.4 ± 0.7	60.8 ± 1.3 (+2.6)
RL Training DAPO*	88.1 ± 4.7	61.4 ± 4.4	82.5 ± 3.4	90.1 ± 7.3	83.9 ± 0.8	69.5 ± 4.9	80.8 ± 1.4	85.9 ± 1.3	73.2 ± 1.3
with EMPG*	97.7 ± 0.8	80.7 ± 6.9	87.5 ± 3.2	87.0 ± 3.6	88.3 ± 4.1	80.0 ± 5.6	88.1 ± 2.1 (+7.3)	86.8 ± 1.9	73.8 ± 1.1 (+0.6)
<i>Base: Qwen2.5-7B-Instruct</i>									
Prompting Qwen2.5	33.4	21.6	19.3	6.9	2.8	3.2	14.8	26.4	7.8
Prompting ReAct	48.5	35.4	34.3	13.2	18.2	17.6	31.2	46.2	19.5
Prompting Reflexion	62.0	41.6	44.9	30.9	36.3	23.8	42.7	58.1	28.8
RL Training PPO (with critic)	92.3	64.0	92.5	89.5	80.3	68.8	80.4	81.4	68.7
RL Training RLOO	87.6	78.2	87.3	81.3	71.9	48.9	75.5	80.3	65.7
RL Training GRPO*	88.8 ± 5.6	43.7 ± 8.2	88.1 ± 3.5	70.3 ± 6.9	77.7 ± 2.3	56.8 ± 9.4	74.8 ± 3.1	77.8 ± 1.4	65.6 ± 1.0
with EMPG*	92.9 ± 2.9	75.2 ± 3.8	74.8 ± 3.9	86.3 ± 4.7	73.7 ± 2.6	65.3 ± 5.8	78.5 ± 1.7 (+3.7)	81.0 ± 1.4	69.3 ± 0.5 (+3.7)
RL Training DAPO*	98.9 ± 1.4	86.1 ± 7.1	94.9 ± 1.6	83.2 ± 6.4	81.4 ± 2.6	90.1 ± 2.2	90.0 ± 1.1	90.6 ± 0.5	79.6 ± 0.6
with EMPG*	99.0 ± 0.3	86.8 ± 5.5	97.3 ± 0.9	94.9 ± 3.9	75.8 ± 3.4	90.3 ± 3.1	91.6 ± 0.8 (+1.6)	92.0 ± 1.2	82.7 ± 1.0 (+3.1)

398 Table 2: Main results on Deep Search tasks, categorized by domain. EMPG demonstrates strong
 399 performance on both in-domain (ID) and out-of-domain (OOD) datasets, with a particularly notable
 400 gain in generalization to OOD tasks.

Method	In-domain (ID)				Out-of-domain (OOD)			Overall	
	WebWalker	HotpotQA	2wiki	Avg.	Musique	Bamboogle	Avg.	Avg.	Avg.
Qwen2.5-32B-Instruct									
DAPO (Baseline)	55.1	66.4	68.9	63.5	38.8	80.8	59.8	62.0	
<i>Ablation Studies</i>									
+ Gradient Scaling	54.9	68.8	67.4	63.7	41.0	86.4	63.7	63.7	
+ Future Bonus	60.6	69.7	67.9	66.1	40.4	82.4	61.4	64.2	
+ EMPG (Ours)	57.5	71.2	71.0	66.6	41.8	84.8	63.7	65.3	
Gain vs. Baseline	(+2.4)	(+4.8)	(+2.1)	(+3.1)	(+3.0)	(+4.0)	(+3.9)	(+3.3)	

411 testing on out-of-domain tasks, where the model faces novel inputs that induce high uncertainty.
 412 Because the policy has learned not to overreact in such situations, it exhibits superior generalization,
 413 providing a robust gain of +3.9 points on OOD tasks. This demonstrates that EMPG is not merely
 414 overfitting; instead, by learning a fundamental skill of how to handle uncertainty, it acquires a more
 415 resilient problem-solving approach that generalizes effectively. Crucially, the full EMPG model,
 416 which integrates both mechanisms, demonstrates a powerful synergy: the model learns to efficiently
 417 exploit known patterns while being robust to novel ones.

418 **Enhancing Training Stability.** Beyond improving sample efficiency, EMPG also significantly
 419 enhances the stability and robustness of the training process. A common failure mode in online
 420 RL fine-tuning is “policy collapse,” where the agent’s policy diverges late in training, leading to a
 421 catastrophic drop in performance. We visualize this phenomenon by tracking the KL Loss during
 422 training, as shown in Figure 2. The DAPO baseline agent initially learns effectively, but its KL
 423 Loss becomes highly erratic after approximately 240 training steps, indicating severe instability.
 424 In contrast, the EMPG-enhanced agent maintains a low and stable KL Loss throughout the entire
 425 training run. This demonstrates that EMPG’s mechanisms, particularly the self-calibrating gradient
 426 scaling, effectively regularize the policy updates, preventing the overly aggressive changes that can
 427 lead to divergence and ensuring a more reliable convergence to a high-performance policy. To ensure
 428 a fair comparison, we select the checkpoint at 220 steps for both the baseline and EMPG for final
 429 evaluation. Despite this, our method could continue to improve its performance with further training.

430 **Step-Level vs. Token-Level Entropy Dynamics.** Our work diverges from prior analyses (Wang
 431 et al., 2025) by focusing on entropy at the “reason-act” step level rather than the token level. To

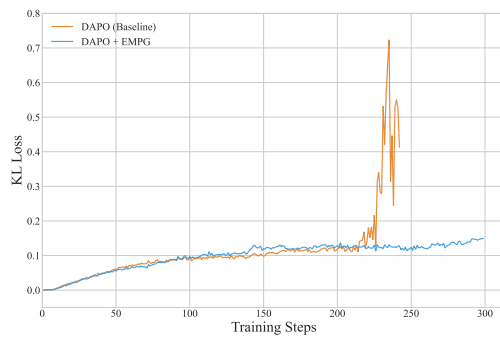


Figure 2: KL Loss dynamics during training for the Qwen2.5-32B-Instruct model. The DAPO baseline (orange) suffers from late-stage instability, evidenced by the sharp, erratic spike in KL Loss. The EMPG-enhanced model (blue) remains stable throughout, showcasing its robustness.

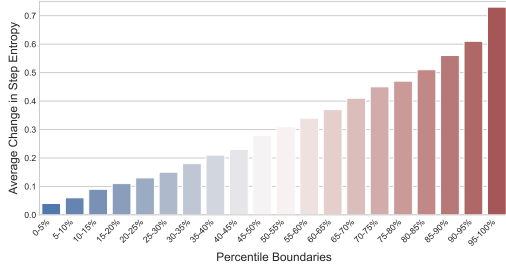


Figure 3: Average entropy change after RL fine-tuning within each 5% entropy percentile range. Unlike token-level findings, even low-entropy steps undergo significant changes, validating our step-level analysis.

validate this choice, we investigate whether the token-level observation—that RL updates primarily affect high-entropy tokens—holds at the step level. We analyze over 9,000 steps on ALFWorld and plot the average entropy change for steps, binned by their initial entropy percentile (Figure 3). Our findings are significant: unlike at the token level, even steps with very low initial entropy (e.g., the 15%-20% percentile) still undergo substantial average entropy changes. This shows the dynamics do not transfer; a confident step can still require significant policy updates. This key finding underscores the importance of our step-centric approach and motivates the design of EMPG to modulate updates across the entire confidence spectrum.

Analysis of Learning Dynamics. An analysis of the learning dynamics, presented in Figure F.1, reveals EMPG’s critical role in overcoming the performance limitations of baseline methods. Across all experiments on both the ALFWorld and WebShop benchmarks, the baseline agents consistently reach a distinct performance plateau, where their learning stagnates and the success rate ceases to improve. In stark contrast, the EMPG-enhanced agents decisively break through this performance ceiling. By providing a richer and more effective learning signal, EMPG enables the agents to sustain their learning momentum, pushing beyond the baseline’s peak and ultimately converging to a significantly higher final success rate. This demonstrates that EMPG is not just accelerating learning, but is fundamentally guiding the agent to discover superior policies that are otherwise inaccessible, effectively escaping the local optima where the baseline methods become trapped.

6 CONCLUSION

In this work, we introduced Entropy-Modulated Policy Gradients (EMPG), a novel and principled framework to alleviate the long-standing credit assignment problem in long-horizon LLM agent training. By leveraging the intrinsic uncertainty of the agent’s “reasoning-action” steps, EMPG dynamically re-calibrates the policy gradient, moving beyond the limitations of sparse, end-of-task rewards. Our method directly addresses the dual challenges of standard policy gradients: it amplifies updates for confident and correct actions, strongly penalizes confident but incorrect steps, and attenuates updates for uncertain steps to promote stability. Through comprehensive experiments on challenging long-horizon benchmarks, including WebShop, ALFWorld, and Deep Search, we demonstrated substantial performance gains over strong baselines like GRPO and DAPO. More fundamentally, our work addresses a key optimization challenge inherent in policy gradient methods operating over high-dimensional, sequential generative policies (such as Large Language Models): the “entropy-gradient coupling” problem. We frame EMPG as a robust and adaptive policy optimization technique for these agents, designed to dynamically assign credit by utilizing the policy’s own intrinsic uncertainty as a reliable, step-level signal.

486 Our findings suggest that an agent’s intrinsic uncertainty is a powerful, yet underexplored, signal
 487 for self-supervision in complex decision-making processes. EMPG provides a scalable alternative
 488 to costly process-based reward models, forging a dense, informative learning signal from minimal
 489 external feedback. For future work, we plan to explore the application of EMPG to other long-
 490 horizon tasks, such as embodied AI and multi-agent collaboration. We believe that this work lays a
 491 foundational stone for developing more efficient, robust, and self-correcting autonomous agents.
 492

493 ETHICS STATEMENT

495 We confirm that this work adheres to the ICLR Code of Ethics. This research focuses on fundamental
 496 algorithms for improving the training efficiency of LLM agents. Our experiments are based entirely
 497 on publicly available models and datasets and do not involve any private data. The authors are fully
 498 responsible for the content and integrity of this research.
 499

500 REPRODUCIBILITY STATEMENT

502 We are committed to ensuring the full reproducibility of this research. All experiments are based on
 503 the publicly available models and public benchmarks. We provide all necessary hyperparameters,
 504 computational environments, and pseudocode for the core logic in the appendix of our paper, and key
 505 results are reported as averages over multiple random seeds to ensure stability.
 506

507 REFERENCES

509 Shivam Agarwal, Zimin Zhang, Lifan Yuan, Jiawei Han, and Hao Peng. The unreasonable effectiveness
 510 of entropy minimization in llm reasoning. *arXiv preprint arXiv:2505.15134*, 2025.

512 Salaheddin Alzubi, Creston Brooks, Purva Chiniya, Edoardo Contente, Chiara von Gerlach, Lu-
 513 cas Irwin, Yihan Jiang, Arda Kaz, Windsor Nguyen, Sewoong Oh, et al. Open deep search:
 514 Democratizing search with open-source reasoning agents. *arXiv preprint arXiv:2503.20201*, 2025.

515 Minghan Chen, Guikun Chen, Wenguan Wang, and Yi Yang. Seed-grpo: Semantic entropy enhanced
 516 grpo for uncertainty-aware policy optimization. *arXiv preprint arXiv:2505.12346*, 2025.

518 Daixuan Cheng, Shaohan Huang, Xuekai Zhu, Bo Dai, Wayne Xin Zhao, Zhenliang Zhang, and Furu
 519 Wei. Reasoning with exploration: An entropy perspective. *arXiv preprint arXiv:2506.14758*, 2025.

521 Xiang Deng, Yu Gu, Boyuan Zheng, Shijie Chen, Sam Stevens, Boshi Wang, Huan Sun, and Yu Su.
 522 Mind2web: Towards a generalist agent for the web. In *Advances in Neural Information Processing
 523 Systems*, 2023.

524 Lang Feng, Zhenghai Xue, Tingcong Liu, and Bo An. Group-in-group policy optimization for llm
 525 agent training. *arXiv preprint arXiv:2505.10978*, 2025.

526 Zitian Gao, Lynx Chen, Joey Zhou, and Bryan Dai. One-shot entropy minimization. *arXiv preprint
 527 arXiv:2505.20282*, 2025.

529 Yichen He, Guanhua Huang, Peiyuan Feng, Yuan Lin, Yuchen Zhang, Hang Li, et al. Pasa: An llm
 530 agent for comprehensive academic paper search. *arXiv preprint arXiv:2501.10120*, 2025.

532 Xanh Ho, Anh-Khoa Duong Nguyen, Saku Sugawara, and Akiko Aizawa. Constructing a multi-hop
 533 qa dataset for comprehensive evaluation of reasoning steps. *arXiv preprint arXiv:2011.01060*,
 534 2020.

535 Bowen Jin, Hansi Zeng, Zhenrui Yue, Jinsung Yoon, Sercan Arik, Dong Wang, Hamed Zamani, and
 536 Jiawei Han. Search-r1: Training llms to reason and leverage search engines with reinforcement
 537 learning. *arXiv preprint arXiv:2503.09516*, 2025.

538 Mandar Joshi, Eunsol Choi, Daniel S Weld, and Luke Zettlemoyer. Triviaqa: A large scale distantly
 539 supervised challenge dataset for reading comprehension. *arXiv preprint arXiv:1705.03551*, 2017.

540 Amirhossein Kazemnejad, Milad Aghajohari, Eva Portelance, Alessandro Sordoni, Siva Reddy, Aaron
 541 Courville, and Nicolas Le Roux. Vineppo: Accurate credit assignment in rl for llm mathematical
 542 reasoning. In *The 4th Workshop on Mathematical Reasoning and AI at NeurIPS'24*, 2024.

543

544 Alexander S Klyubin, Daniel Polani, and Chrystopher L Nehaniv. Empowerment: A universal
 545 agent-centric measure of control. In *IEEE Congress on Evolutionary Computation*, 2005.

546

547 Tom Kwiatkowski, Jennimaria Palomaki, Olivia Redfield, Michael Collins, Ankur Parikh, Chris
 548 Alberti, Danielle Epstein, Illia Polosukhin, Jacob Devlin, Kenton Lee, et al. Natural questions: a
 549 benchmark for question answering research. *Transactions of the Association for Computational
 550 Linguistics*, 2019.

551

552 Xiaoxi Li, Guanting Dong, Jiajie Jin, Yuyao Zhang, Yujia Zhou, Yutao Zhu, Peitian Zhang, and
 553 Zhicheng Dou. Search-o1: Agentic search-enhanced large reasoning models. *arXiv preprint
 554 arXiv:2501.05366*, 2025.

555

556 Yingru Li. Logit dynamics in softmax policy gradient methods. *arXiv preprint arXiv:2506.12912*,
 557 2025.

558

559 Hunter Lightman, Vineet Kosaraju, Yuri Burda, Harrison Edwards, Bowen Baker, Teddy Lee, Jan
 560 Leike, John Schulman, Ilya Sutskever, and Karl Cobbe. Let's verify step by step. In *International
 561 Conference on Learning Representations*, 2023.

562

563 Jiacai Liu, Chaojie Wang, Chris Yuhao Liu, Liang Zeng, Rui Yan, Yiwen Sun, Yang Liu, and Yahui
 564 Zhou. Improving multi-step reasoning abilities of large language models with direct advantage
 565 policy optimization. *arXiv preprint arXiv:2412.18279*, 2024.

566

567 Alfréd Rényi. On measures of entropy and information. In *Proceedings of the fourth Berkeley
 568 symposium on mathematical statistics and probability, volume 1: contributions to the theory of
 569 statistics*, 1961.

570

571 John Schulman, Filip Wolski, Prafulla Dhariwal, Alec Radford, and Oleg Klimov. Proximal policy
 572 optimization algorithms. *arXiv preprint arXiv:1707.06347*, 2017.

573

574 ByteDance Seed, Jiaze Chen, Tiantian Fan, Xin Liu, Lingjun Liu, Zhiqi Lin, Mingxuan Wang,
 575 Chengyi Wang, Xiangpeng Wei, Wenyuan Xu, et al. Seed1. 5-thinking: Advancing superb
 576 reasoning models with reinforcement learning. *arXiv preprint arXiv:2504.13914*, 2025.

577

578 Zhihong Shao, Peiyi Wang, Qihao Zhu, Runxin Xu, Junxiao Song, Xiao Bi, Haowei Zhang,
 579 Mingchuan Zhang, YK Li, Yang Wu, et al. Deepseekmath: Pushing the limits of mathematical
 580 reasoning in open language models. *arXiv preprint arXiv:2402.03300*, 2024.

581

582 Guangming Sheng, Chi Zhang, Zilingfeng Ye, Xibin Wu, Wang Zhang, Ru Zhang, Yanghua Peng,
 583 Haibin Lin, and Chuan Wu. Hybridflow: A flexible and efficient rlhf framework. *arXiv preprint
 584 arXiv: 2409.19256*, 2024.

585

586 Mohit Shridhar, Xingdi Yuan, Marc-Alexandre Cote, Yonatan Bisk, Adam Trischler, and Matthew
 587 Hausknecht. Alfworld: Aligning text and embodied environments for interactive learning. In
 588 *International Conference on Learning Representations*, 2021.

589

590 Abdullah Vanlioglu. Entropy-guided sequence weighting for efficient exploration in rl-based llm
 591 fine-tuning. *arXiv preprint arXiv:2503.22456*, 2025.

592

593 Shenzhi Wang, Le Yu, Chang Gao, Chujie Zheng, Shixuan Liu, Rui Lu, Kai Dang, Xionghui Chen,
 594 Jianxin Yang, Zhenru Zhang, Yuqiong Liu, An Yang, Andrew Zhao, Yang Yue, Shiji Song, Bowen
 595 Yu, Gao Huang, and Junyang Lin. Beyond the 80/20 rule: High-entropy minority tokens drive
 596 effective reinforcement learning for llm reasoning. *arXiv preprint arXiv:2506.01939*, 2025.

597

598 Jason Wei, Xuezhi Wang, Dale Schuurmans, Maarten Bosma, Fei Xia, Ed Chi, Quoc V Le, Denny
 599 Zhou, et al. Chain-of-thought prompting elicits reasoning in large language models. In *Advances
 600 in neural information processing systems*, 2022.

594 Yuxiang Wei, Olivier Duchenne, Jade Copet, Quentin Carbonneaux, Lingming Zhang, Daniel Fried,
 595 Gabriel Synnaeve, Rishabh Singh, and Sida I Wang. Swe-rl: Advancing llm reasoning via
 596 reinforcement learning on open software evolution. *arXiv preprint arXiv:2502.18449*, 2025a.
 597

598 Zhepei Wei, Wenlin Yao, Yao Liu, Weizhi Zhang, Qin Lu, Liang Qiu, Changlong Yu, Puyang
 599 Xu, Chao Zhang, Bing Yin, et al. Webagent-r1: Training web agents via end-to-end multi-turn
 600 reinforcement learning. *arXiv preprint arXiv:2505.16421*, 2025b.

601 Jialong Wu, Wenbiao Yin, Yong Jiang, Zhenglin Wang, Zekun Xi, Runnan Fang, Linhai Zhang,
 602 Yulan He, Deyu Zhou, Pengjun Xie, et al. Webwalker: Benchmarking llms in web traversal. *arXiv
 603 preprint arXiv:2501.07572*, 2025.

604 An Yan, Zhengyuan Yang, Wanrong Zhu, Kevin Lin, Linjie Li, Jianfeng Wang, Jianwei Yang, Yiwu
 605 Zhong, Julian McAuley, Jianfeng Gao, et al. Gpt-4v in wonderland: Large multimodal models for
 606 zero-shot smartphone gui navigation. *arXiv preprint arXiv:2311.07562*, 2023.

607 Qwen An Yang, Baosong Yang, Beichen Zhang, Binyuan Hui, Bo Zheng, Bowen Yu, Chengyuan
 608 Li, Dayiheng Liu, Fei Huang, Guanting Dong, Haoran Wei, Huan Lin, Jian Yang, Jianhong Tu,
 609 Jianwei Zhang, Jianxin Yang, Jiaxin Yang, Jingren Zhou, Junyang Lin, Kai Dang, Keming Lu,
 610 Keqin Bao, Kexin Yang, Le Yu, Mei Li, Mingfeng Xue, Pei Zhang, Qin Zhu, Rui Men, Runji Lin,
 611 Tianhao Li, Tingyu Xia, Xingzhang Ren, Xuancheng Ren, Yang Fan, Yang Su, Yi-Chao Zhang,
 612 Yunyang Wan, Yuqi Liu, Zeyu Cui, Zhenru Zhang, Zihan Qiu, Shanghaoran Quan, and Zekun
 613 Wang. Qwen2.5 technical report. *arXiv preprint arXiv:2412.15115*, 2024.

614 Zhilin Yang, Peng Qi, Saizheng Zhang, Yoshua Bengio, William W Cohen, Ruslan Salakhutdinov,
 615 and Christopher D Manning. Hotpotqa: A dataset for diverse, explainable multi-hop question
 616 answering. *arXiv preprint arXiv:1809.09600*, 2018.

617 Shunyu Yao, Howard Chen, John Yang, and Karthik Narasimhan. Webshop: Towards scalable
 618 real-world web interaction with grounded language agents. In *Advances in Neural Information
 619 Processing Systems*, 2022.

620 Shunyu Yao, Jeffrey Zhao, Dian Yu, Nan Du, Izhak Shafran, Karthik Narasimhan, and Yuan Cao.
 621 React: Synergizing reasoning and acting in language models. In *International Conference on
 622 Learning Representations*, 2023.

623 Qiying Yu, Zheng Zhang, Ruofei Zhu, Yufeng Yuan, Xiaochen Zuo, Yu Yue, Tiantian Fan, Gaohong
 624 Liu, Lingjun Liu, Xin Liu, Haibin Lin, Zhiqi Lin, Bole Ma, Guangming Sheng, Yuxuan Tong, Chi
 625 Zhang, Mofan Zhang, Wang Zhang, Hang Zhu, Jinhua Zhu, Jiaze Chen, Jiangjie Chen, Chengyi
 626 Wang, Honglin Yu, Weinan Dai, Yuxuan Song, Xiang Wei, Haodong Zhou, Jingjing Liu, Wei Ma,
 627 Ya-Qin Zhang, Lin Yan, Mu Qiao, Yong-Xu Wu, and Mingxuan Wang. Dapo: An open-source llm
 628 reinforcement learning system at scale. *arXiv preprint arXiv:2503.14476*, 2025.

629 Kechi Zhang, Jia Li, Ge Li, Xianjie Shi, and Zhi Jin. Codeagent: Enhancing code generation
 630 with tool-integrated agent systems for real-world repo-level coding challenges. *arXiv preprint
 631 arXiv:2401.07339*, 2024.

632 Kongcheng Zhang, Qi Yao, Shunyu Liu, Yingjie Wang, Baisheng Lai, Jieping Ye, Mingli Song,
 633 and Dacheng Tao. Consistent paths lead to truth: Self-rewarding reinforcement learning for llm
 634 reasoning. *arXiv preprint arXiv:2506.08745*, 2025a.

635 Qingyang Zhang, Haitao Wu, Changqing Zhang, Peilin Zhao, and Yatao Bian. Right question
 636 is already half the answer: Fully unsupervised llm reasoning incentivization. *arXiv preprint
 637 arXiv:2504.05812*, 2025b.

638 Xingjian Zhang, Siwei Wen, Wenjun Wu, and Lei Huang. Edge-grpo: Entropy-driven grpo with
 639 guided error correction for advantage diversity. *arXiv preprint arXiv:2507.21848*, 2025c.

640 Yue Zhang, Yafu Li, Leyang Cui, Deng Cai, Lemao Liu, Tingchen Fu, Xinting Huang, Enbo Zhao,
 641 Yu Zhang, Yulong Chen, et al. Siren’s song in the ai ocean: A survey on hallucination in large
 642 language models. *Computational Linguistics*, pp. 1–45, 2025d.

643 Xuandong Zhao, Zhewei Kang, Aosong Feng, Sergey Levine, and Dawn Song. Learning to reason
 644 without external rewards. *arXiv preprint arXiv:2505.19590*, 2025.

648 Yuxiang Zheng, Dayuan Fu, Xiangkun Hu, Xiaojie Cai, Lyumanshan Ye, Pengrui Lu, and Pengfei
649 Liu. Deepresearcher: Scaling deep research via reinforcement learning in real-world environments.
650 *arXiv preprint arXiv:2504.03160*, 2025.

651 Yuxin Zuo, Kaiyan Zhang, Li Sheng, Shang Qu, Ganqu Cui, Xuekai Zhu, Haozhan Li, Yuchen
652 Zhang, Xinwei Long, Ermo Hua, et al. Ttrl: Test-time reinforcement learning. *arXiv preprint*
653 *arXiv:2504.16084*, 2025.

654

655

656

657

658

659

660

661

662

663

664

665

666

667

668

669

670

671

672

673

674

675

676

677

678

679

680

681

682

683

684

685

686

687

688

689

690

691

692

693

694

695

696

697

698

699

700

701

702 **A LLM USAGE DISCLOSURE**
703704 We used large language models as a writing assistant to polish and improve the clarity of the English
705 language in this manuscript. The model was not used to generate any core content, including research
706 ideas, experimental results, or technical analysis. All authors have reviewed and are fully responsible
707 for the final content of the paper.
708709 **B DETAILED PRELIMINARIES**
710711 **B.1 POLICY OPTIMIZATION IN REINFORCEMENT LEARNING**
712713 Our work is grounded in policy gradient methods, which seek to optimize a policy π_θ parameterized
714 by θ to maximize the expected reward objective:
715

716
$$\mathcal{J}(\pi_\theta) := \mathbb{E}_{\tau \sim \pi_\theta}[R(\tau)] \quad (10)$$

717 where τ is a trajectory sampled under policy π_θ and $R(\tau)$ is its total return. The policy gradient
718 theorem allows for direct optimization of this objective via gradient ascent. The gradient is estimated
719 as an expectation over trajectories:
720

721
$$\nabla_\theta \mathcal{J}(\pi_\theta) = \mathbb{E}_{\tau \sim \pi_\theta} \left[\sum_{t=0}^T A(s_t, a_t) \nabla_\theta \log \pi_\theta(a_t | s_t) \right] \quad (11)$$

722

723 where s_t and a_t are the state and action at time step t , respectively.
724725 A key challenge in estimating this gradient is its inherently high variance. To mitigate this, an
726 advantage function, $A(s_t, a_t)$, is used to measure the relative quality of an action. This advantage is
727 typically estimated using a learned value model, which predicts the expected return from a given state
728 (Schulman et al., 2017). However, this approach has significant drawbacks. The value model is often
729 comparable in size to the policy model, introducing substantial memory and computational overhead.
730 Furthermore, the effectiveness of the algorithm hinges on the reliability of its value estimates, which
731 are inherently difficult to learn accurately Liu et al. (2024); Kazemnejad et al. (2024), especially
732 for complex tasks with long response horizons. Due to these challenges, value-free methods, which
733 estimate the advantage directly from sampled trajectories without a learned value function, have
734 become increasingly popular (Shao et al., 2024; Yu et al., 2025). Our work is also grounded in this
735 value-free paradigm, foregoing a value model to improve training efficiency and stability.
736737 **B.2 RL FRAMEWORK FOR LONG-HORIZON AGENT TASKS**
738739 We formalize the long-horizon task as a standard reinforcement learning problem. An LLM agent
740 interacts with an environment over a trajectory $\tau = (s_0, a_0, r_0, \dots, s_T, a_T, r_T)$. The reward signal
741 is sparse, with $r_t = 0$ for all non-terminal steps. Assuming an undiscounted setting ($\gamma = 1$), the
742 trajectory return $R(\tau)$ is thus determined solely by the final outcome:
743

744
$$R(\tau) = \sum_{t=0}^T \gamma^t r_t = r_T \in \{0, 1\} \quad (12)$$

745

746 In our work, a single step corresponds to a complete "reason-then-act" cycle (e.g., as in ReAct (Yao
747 et al., 2023)), forming a multi-step decision-making process. This sparse-reward, long-horizon setting
748 epitomizes two fundamental RL challenges: the **credit assignment problem** and the **exploration
749 problem**.
750751 **B.3 STRATEGIES FOR LEARNING FROM SPARSE OUTCOME-BASED REWARDS**
752753 To enable effective learning from sparse, outcome-based rewards in long-horizon tasks, several
754 powerful strategies have emerged that form the foundation of modern LLM RL.
755

- **Trust Region Learning.** Proximal Policy Optimization (PPO) (Schulman et al., 2017) serves as the bedrock algorithm. Its primary innovation is not credit assignment, but ensuring

756 training stability. It achieves this by constraining policy updates within a trust region, using
 757 a clipped objective on the probability ratio $\rho_t(\theta) = \frac{\pi_\theta(a_t|s_t)}{\pi_{\theta_{\text{old}}}(a_t|s_t)}$. When applied to sparse
 758 reward tasks, PPO's effectiveness fundamentally depends on the quality of its advantage
 759 estimates, which implicitly perform the task of credit assignment Kazemnejad et al. (2024).
 760

761 • **Group-Based Advantage Estimation.** Group Relative Policy Optimization (GRPO) (Shao
 762 et al., 2024) builds upon this foundation with a direct solution for credit assignment. It
 763 addresses the high variance of the policy gradient inherent in sparse rewards by sampling
 764 multiple responses (M) and computing a Z-score-like advantage:

$$766 \quad A_{ij} = \frac{r(x_i, y_{ij}) - \text{mean}_{k=1}^M(r(x_i, y_{ik}))}{\text{std}_{k=1}^M(r(x_i, y_{ik})) + \epsilon} \quad (13)$$

769 Here, $r(x_i, y_{ij})$ is the final outcome-based reward for the j -th response, and ϵ is a small
 770 constant added for numerical stability. This comparative evaluation effectively identifies the
 771 best-in-batch responses, providing a robust signal.
 772

773 • **Adaptive Data Curation.** Decoupled Clip and Dynamic Sampling Policy Optimization
 774 (DAPO) (Yu et al., 2025) further refines the learning process by curating the data itself. It
 775 addresses failure modes in GRPO by filtering and resampling trajectories to form more
 776 informative training batches. By focusing updates on a buffer of high-quality samples, it
 777 improves the efficiency of learning from the sparse reward signal.
 778

779 While powerful, these strategies share a common reliance on processing external, outcome-based
 780 reward signals. As they are primarily designed for single-turn generation, they treat entire action
 781 sequences as monolithic blocks. When applied to interactive agent tasks, this leads to a coarse,
 782 trajectory-level credit assignment that fails to pinpoint which specific actions in a long sequence
 783 were critical for success. This approach ignores the rich, intrinsic signals available at each step of
 784 the generative process. Our work diverges by proposing a new paradigm that peers inside the model,
 785 leveraging its intrinsic, step-wise uncertainty.

787 C PROOF OF PROPOSITION 1

789 We aim to prove that $\mathbb{E}_{a_k \sim \pi} [||\nabla_z \log \pi_k||^2] = 1 - \sum_{j=1}^{|V|} \pi_j^2$. The proof requires the result for the
 790 gradient norm of a single action a_k , which we state as a lemma.
 791

792 **Lemma.** The squared L2-norm of the score function with respect to the logits, for a chosen action
 793 a_k , is given by: $||\nabla_z \log \pi_k||^2 = 1 - 2\pi_k + \sum_{j=1}^{|V|} \pi_j^2$.
 794

797 *Proof of Lemma.* Let the logits be $z = (z_1, \dots, z_{|V|})$. The policy is $\pi_k = \exp(z_k) / \sum_j \exp(z_j)$.
 798 The partial derivative of the log-probability $\log \pi_k$ with respect to an arbitrary logit z_i is $\frac{\partial \log \pi_k}{\partial z_i} =$
 799 $\delta_{ik} - \pi_i$, where δ_{ik} is the Kronecker delta. The squared L2-norm of the gradient vector $\nabla_z \log \pi_k$ is
 800 therefore:
 801

$$802 \quad ||\nabla_z \log \pi_k||^2 = \sum_{i=1}^{|V|} (\delta_{ik} - \pi_i)^2 = (1 - \pi_k)^2 + \sum_{i \neq k} (-\pi_i)^2$$

$$803 \quad = (1 - 2\pi_k + \pi_k^2) + \sum_{i \neq k} \pi_i^2 = 1 - 2\pi_k + \sum_{j=1}^{|V|} \pi_j^2$$

810 *Proof of Proposition 1.* The expectation is taken over all possible choices of action a_k according to
 811 the policy distribution π . Using the result from the lemma:

$$\begin{aligned}
 813 \quad \mathbb{E}_{k \sim \pi} [||\nabla_z \log \pi_k||^2] &= \sum_{k=1}^{|V|} \pi_k \cdot (||\nabla_z \log \pi_k||^2) \\
 814 &= \sum_{k=1}^{|V|} \pi_k \left(1 - 2\pi_k + \sum_{j=1}^{|V|} \pi_j^2 \right) \\
 815 &= \sum_{k=1}^{|V|} \pi_k - 2 \sum_{k=1}^{|V|} \pi_k^2 + \sum_{k=1}^{|V|} \pi_k \left(\sum_{j=1}^{|V|} \pi_j^2 \right) \\
 816 &= 1 - 2 \sum_{k=1}^{|V|} \pi_k^2 + \left(\sum_{j=1}^{|V|} \pi_j^2 \right) \left(\sum_{k=1}^{|V|} \pi_k \right) \quad (\text{Factor out constant term}) \\
 817 &= 1 - 2 \sum_{k=1}^{|V|} \pi_k^2 + \left(\sum_{j=1}^{|V|} \pi_j^2 \right) \cdot 1 \\
 818 &= 1 - \sum_{k=1}^{|V|} \pi_k^2
 \end{aligned}$$

819 Recalling the definition of Rényi entropy of order 2, $H_2(\pi) = -\log(\sum_{j=1}^{|V|} \pi_j^2)$, we can identify the
 820 term $\sum \pi_j^2$ as the collision probability, which is equivalent to $\exp(-H_2(\pi))$. Substituting this into
 821 our result yields the final information-theoretic form:

$$822 \quad \mathbb{E}_{k \sim \pi} [||\nabla_z \log \pi_k||^2] = 1 - \exp(-H_2(\pi))$$

823 This completes the proof of the proposition. ■

824 D THEORETICAL FOUNDATION OF THE EMPG UPDATE RULE

825 In this section, we provide a rigorous theoretical justification for the Entropy-Modulated Policy
 826 Gradients (EMPG) algorithm. We demonstrate that the EMPG update rule can be formally derived as
 827 the gradient of a composite objective function, $J_{\text{EMPG}}(\theta)$. This interpretation substantiates that EMPG
 828 is a principled optimization method that reshapes the standard reinforcement learning objective to
 829 favor policies that are both effective and robust.

830 D.1 THE STANDARD POLICY GRADIENT OBJECTIVE

831 We begin with the standard objective in policy-based reinforcement learning, which is to maximize
 832 the expected total return. In the context of sparse, outcome-based rewards, this objective simplifies to
 833 maximizing the expected advantage (return) of a trajectory τ :

$$834 \quad J(\theta) = \mathbb{E}_{\tau \sim \pi_\theta} [A^{(\tau)}] \tag{14}$$

835 where $A^{(\tau)}$ is the scalar return for a trajectory τ sampled from the policy π_θ . The gradient of this
 836 objective is given by the Policy Gradient Theorem:

$$837 \quad \nabla_\theta J(\theta) = \mathbb{E}_{\tau \sim \pi_\theta} \left[\left(\sum_{t=0}^{T-1} \nabla_\theta \log \pi_\theta(a_t | s_t) \right) A^{(\tau)} \right] \tag{15}$$

838 For any single trajectory τ , the gradient estimator is $\mathcal{G}^{(\tau)}(\theta) = A^{(\tau)} \sum_{t=0}^{T-1} \nabla_\theta \log \pi_\theta(a_t | s_t)$. This
 839 formulation reveals the core issue identified in Proposition 1: the contribution of each step's score
 840 function, $\nabla_\theta \log \pi_\theta(a_t | s_t)$, is weighted uniformly by the trajectory's outcome $A^{(\tau)}$, while its norm is
 841 intrinsically coupled with the policy entropy H_t .

864 D.2 THE EMPG COMPOSITE OBJECTIVE FUNCTION
865

866 We posit that EMPG performs gradient ascent on a composite objective function $J_{\text{EMPG}}(\theta)$. This ob-
867 jective augments the standard RL objective with a term that explicitly accounts for policy uncertainty,
868 thereby decoupling the learning signal’s magnitude and direction from the policy’s raw confidence.
869 We define this objective as:

$$870 \quad J_{\text{EMPG}}(\theta) = J_{\text{extrinsic}}(\theta) + J_{\text{intrinsic}}(\theta) \quad (16)$$

872 Here, $J_{\text{extrinsic}}(\theta)$ is a re-weighted extrinsic objective that addresses the gradient *magnitude* problem,
873 and $J_{\text{intrinsic}}(\theta)$ is an intrinsic objective that guides the policy’s *direction* towards states of higher
874 certainty.

876 D.2.1 THE RE-WEIGHTED EXTRINSIC OBJECTIVE
877

878 The self-calibrating gradient scaling component of EMPG, $A^{(\tau)} \cdot \mathcal{H}$, can be interpreted as performing
879 an update on a modified extrinsic objective. Formally, we define a state-dependent weighting function
880 $\omega(s_t, \theta) = \mathcal{H}$, which is a function of the policy’s entropy at state s_t . The gradient update for this
881 component is:

$$882 \quad \mathcal{G}_{\text{extrinsic}}^{(\tau)}(\theta) = \sum_{t=0}^{T-1} A^{(\tau)} \cdot \omega(s_t^{(\tau)}, \theta) \cdot \nabla_{\theta} \log \pi_{\theta}(a_t | s_t) \quad (17)$$

885 This formulation is equivalent to optimizing the standard objective $J(\theta)$ under a *state-dependent*
886 *measure*, where the contribution of each state is re-weighted. While deriving a closed-form objective
887 $J_{\text{extrinsic}}(\theta)$ is non-trivial because ω depends on θ in a complex manner (via batch statistics), this
888 interpretation is sufficient to justify the update rule. The weighting function $\omega(s_t, \theta)$ serves as an
889 adaptive, information-theoretic learning rate that directly counteracts the dynamics described in
890 Proposition 1. It amplifies the learning signal for confident (low-entropy) steps and dampens it for
891 uncertain (high-entropy) steps, thus achieving a direct re-calibration of the gradient’s magnitude.

892 D.2.2 THE INTRINSIC CLARITY OBJECTIVE
893

894 The Future Clarity Bonus can be modeled as the gradient of a well-defined intrinsic objective function.
895 We define an intrinsic reward, r_t^{int} , awarded at step t for transitioning to a state s_{t+1} with high policy
896 clarity:

897 **Definition** (Clarity Reward). The intrinsic clarity reward at step t is a function of the policy entropy
898 at the subsequent state s_{t+1} :

$$900 \quad r_t^{\text{int}}(s_{t+1}; \theta) = \zeta \cdot f(H(\pi_{\theta}(\cdot | s_{t+1}))) = \zeta \cdot \exp(-k' \cdot H_{\text{norm}, t+1}) \quad (18)$$

902 This reward incentivizes actions that lead to predictable future states. The corresponding intrinsic
903 objective, $J_{\text{intrinsic}}(\theta)$, is the expected cumulative intrinsic reward:

$$905 \quad J_{\text{intrinsic}}(\theta) = \mathbb{E}_{\tau \sim \pi_{\theta}} \left[\sum_{t=0}^{T-1} r_t^{\text{int}}(s_{t+1}; \theta) \right] \quad (19)$$

909 Applying the policy gradient theorem to this objective, and using the immediate intrinsic reward as a
910 one-step advantage estimate (a common form of advantage shaping), yields the gradient:

$$912 \quad \nabla_{\theta} J_{\text{intrinsic}}(\theta) = \mathbb{E}_{\tau \sim \pi_{\theta}} \left[\sum_{t=0}^{T-1} (\nabla_{\theta} \log \pi_{\theta}(a_t | s_t)) r_t^{\text{int}}(s_{t+1}; \theta) \right] \quad (20)$$

$$915 \quad = \mathbb{E}_{\tau_i \sim \pi_{\theta}} \left[\sum_{t=0}^{T_i-1} (\nabla_{\theta} \log \pi_{\theta}(a_t | s_t)) \zeta \cdot f(H_{t+1}^{(\tau)}) \right] \quad (21)$$

917 This gradient precisely matches the Future Clarity Bonus component of the EMPG update.

918 D.3 SYNTHESIS: THE FULL EMPG GRADIENT
919920 By combining the gradients of the extrinsic and intrinsic objectives, we recover the full EMPG
921 gradient estimator for a single trajectory τ :

922
$$\mathcal{G}_{\text{EMPG}}^{(\tau)}(\theta) = \mathcal{G}_{\text{extrinsic}}^{(\tau)}(\theta) + \nabla_{\theta} J_{\text{intrinsic}}(\theta)|_{\tau} \quad (22)$$

923

924
$$= \sum_{t=0}^{T-1} A^{(\tau)} \cdot \mathcal{H} \cdot \nabla_{\theta} \log \pi_{\theta}(a_t|s_t) + \sum_{t=0}^{T-1} \zeta \cdot f(H_{t+1}^{(\tau)}) \cdot \nabla_{\theta} \log \pi_{\theta}(a_t|s_t) \quad (23)$$

925

926
$$= \sum_{t=0}^{T-1} \left(A^{(\tau)} \cdot \mathcal{H} + \zeta \cdot f(H_{t+1}^{(\tau)}) \right) \nabla_{\theta} \log \pi_{\theta}(a_t|s_t) \quad (24)$$

927

928 This derivation confirms that the EMPG algorithm performs a principled gradient ascent on the composite
929 objective $J_{\text{EMPG}}(\theta)$. This objective function holistically reshapes the optimization landscape by (1) adaptively scaling the extrinsic reward signal to ensure its magnitude is motivationally salient
930 rather than merely a function of policy entropy, and (2) introducing an intrinsic drive towards robust,
931 predictable solution paths. This dual-pronged approach provides a theoretical foundation for why
932 EMPG successfully mitigates the challenges posed by the inherent dynamics of standard policy
933 gradients.
934935 E EXPERIMENTAL SETTINGS
936937 This appendix provides a detailed description of the experimental settings, hardware configurations,
938 and hyperparameter choices for our experiments across the three main benchmarks. Due to the
939 differences in training frameworks and task environments, the settings for WebShop/ALFWorld and
940 Deep Search are described in separate subsections.
941942 E.1 WEBSHOP AND ALFWORLD EXPERIMENTS
943944 Our experiments on WebShop and ALFWorld are conducted within the **Verl-Agent** framework,
945 an extension of the **veRL** Sheng et al. (2024) training codebase specifically designed for training
946 large language model (LLM) agents via reinforcement learning. Verl-Agent provides a powerful
947 and scalable platform for long-horizon, multi-turn RL training by enabling fully customizable per-
948 step input structures, history management, and memory modules. It supports a diverse set of RL
949 algorithms and a rich suite of agent environments, making it highly suitable for our work.
950951 For a fair comparison, all experiments were re-executed on our hardware platform. While the original
952 experiments were performed using H200 GPUs, our work utilized A100 GPUs due to resource
953 constraints. We observed that the original training scripts for the Qwen2.5-1.5B-Instruct model,
954 designed for $2 \times$ H100, would result in out-of-memory errors on A100s. Therefore, we used $4 \times$
955 A100 GPUs for the 1.5B models and $8 \times$ A100 GPUs for the 7B models. All baselines were re-trained
956 under the same hardware, seeds, and settings to ensure strict comparability. The key hyperparameters
957 for these experiments are summarized in Table 3.
958959 E.2 DEEP SEARCH EXPERIMENTS
960961 Our experiments on the Deep Search task were conducted using an in-house RL training framework.
962 The agent was equipped with two primary tools: Bing Search as the search engine and a web viewer
963 tool capable of reading web page content and summarizing long articles.
964965 A key part of the Deep Search training was the data curation process. We constructed a unique training
966 dataset of 17,000 instances by filtering from a variety of public benchmarks, including WebWalker
967 Wu et al. (2025), HotpotQA Yang et al. (2018), 2WikiMultiHopQA Ho et al. (2020), NaturalQuestions
968 Kwiatkowski et al. (2019), and TriviaQA Joshi et al. (2017). We gratefully acknowledge the initial
969 data collection and preliminary filtering by the DeepResearcher team Zheng et al. (2025). We
970 performed two deeper filtering steps:
9711. **Direct Answer Filtering:** We sampled 5 results per question using Doubao-Seed-1.6
(Thinking) Seed et al. (2025). We then filtered out all questions that could be answered

972
973
974 Table 3: Key Hyperparameters for WebShop and ALFWorld Experiments.
975
976
977
978
979
980
981
982
983
984
985
986
987
988
989
990
991
992
993
994
995
996
997
998
999

Parameter	Value
Actor Learning Rate	1e-6
KL Loss Coefficient	0.01
KL Penalty	low var kl
Entropy Coefficient	0.001
Clip High (DAPPO)	0.28
Clip Low (DAPPO)	0.2
Clip Low/High (GRPO)	0.2
Batch Size	16
Training Step	150
Rollout Group Size	8
Rollout Temperature	1.0
ζ	0.05
k, k'	1.0
Max Actions (ALFWorld)	50
Max Actions (WebShop)	15
History Observation	2
GPUs	4 × A100 (1.5B), 8 × A100 (7B)

directly (where at least one of the 5 results was correct) to ensure the agent learns to use its search tools rather than relying on memorized answers.

2. **Agent Workflow Filtering:** We further filtered the dataset by sampling 8 results using a search workflow built on Doubao-Seed-1.6 (Thinking). We removed data points that were "stably all-correct" to focus the RL training on more challenging instances and improve training efficiency.

1000 The key hyperparameters for the RL training on the Deep Search task are detailed in Table 4.
1001

1002 Table 4: Key Hyperparameters for Deep Search Experiments.
1003

Parameter	Value
Actor Learning Rate	1e-6
KL Loss Coefficient	0.001
KL Penalty	low var kl
Entropy Coefficient	0.0
Clip High	0.28
Clip Low	0.2
Batch Size	64
Training Step	220
Rollout Group Size	16
Rollout Temperature	1.0
ζ	0.1
k, k'	1.0
Max Actions	15
GPUs	32 × A100

1020 F ANALYSIS OF LEARNING DYNAMICS

1021
1022
1023 This section provides a detailed visualization of the learning dynamics, complementing the analysis
1024 in the main body of the paper. Figure F.1 illustrates the training progress of EMPG-enhanced agents
1025 compared to their baseline counterparts (GRPO and DAPPO) on both the WebShop and ALFWorld
benchmarks. As shown in the learning curves, the baseline agents consistently hit a performance

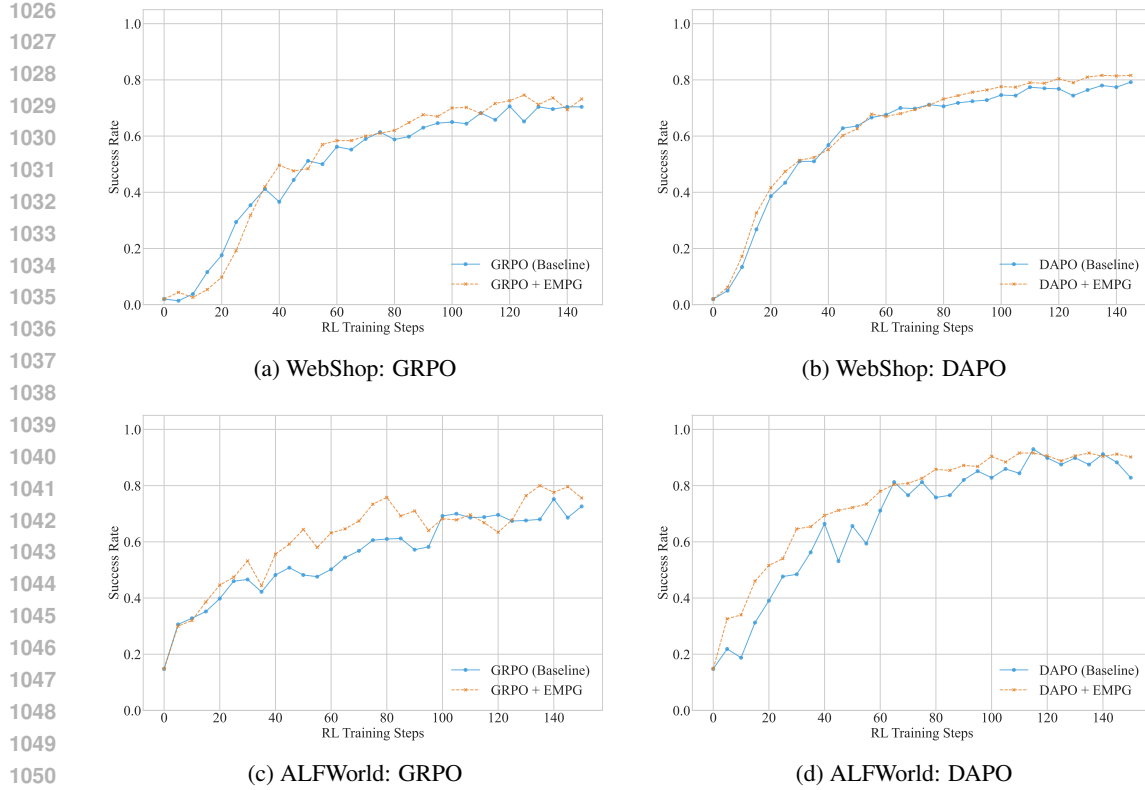


Figure F.1: Learning dynamics comparison for the Qwen2.5-7B-Instruct model on the WebShop and ALFWorld benchmarks (evaluated on the validation set). In all four scenarios, the EMPG-enhanced agents (orange, dashed) demonstrate a superior success rate compared to their respective baselines (blue, solid).

ceiling, with their success rates stagnating early in the training process. In contrast, our EMPG-enhanced agents overcome this plateau, sustaining their learning momentum to achieve significantly higher final success rates across all settings. This evidence supports our central claim that EMPG provides a more effective learning signal, enabling agents to escape the local optima that trap standard policy gradient methods.

G EXPERIMENTAL ANALYSIS FOR ROBUSTNESS

G.1 HYPERPARAMETER SENSITIVITY ANALYSIS

We conducted a thorough sensitivity analysis to ensure the practical robustness of EMPG across its primary hyperparameter settings: the Future Clarity Bonus weight (ζ), and the gradient temperature parameters (k and k'). These experiments were performed on the ALFWorld benchmark using the Qwen2.5-1.5B-Instruct policy trained with GRPO. For simplicity, we set $k = k'$ as both parameters operate on the same normalized step-level entropy, and we report the average success rate over 4 independent runs for each configuration.

Analysis of Hyperparameter Sensitivity. The results in Table 5 confirm that EMPG maintains **stable and competitive performance** across the tested range of hyperparameters ($\zeta \in [0.01, 0.1]$ and $k, k' \in [0.5, 1.5]$).

- **Impact of k and k' :** Varying the temperature k (e.g., from 0.5 to 1.5) results in minimal fluctuation in overall performance (73.1% to 73.8%). This stability is a direct and expected benefit of our *Self-Calibrating Gradient Scaling* design (Eq. 6). Since the scaling is normal-

1080 Table 5: Hyperparameter Sensitivity Analysis of EMPG on ALFWorld (Qwen2.5-1.5B-Instruct +
 1081 GRPO). The method shows strong robustness to variations in ζ and k .

Parameters		ALFWorld Subtask Success Rate (%)						All (%)
ζ	k, k'	Pick	Look	Clean	Heat	Cool	Pick2	Overall
0.01		83.7 \pm 1.2	68.7 \pm 5.3	78.8 \pm 4.0	72.4 \pm 6.8	59.7 \pm 4.5	69.4 \pm 1.9	73.4 \pm 1.9
0.05	1.0	85.5 \pm 4.8	33.5 \pm 6.4	78.9 \pm 2.5	76.2 \pm 9.7	74.7 \pm 1.9	69.1 \pm 6.4	73.7 \pm 2.7
0.1		84.5 \pm 2.0	51.0 \pm 16.2	82.4 \pm 2.1	82.2 \pm 4.5	78.0 \pm 4.3	78.5 \pm 2.7	78.5 \pm 1.2
	0.5	82.7 \pm 1.5	51.1 \pm 3.1	77.8 \pm 1.9	74.8 \pm 3.9	68.2 \pm 5.5	70.2 \pm 1.5	73.1 \pm 1.3
0.05	1.0	85.5 \pm 4.8	33.5 \pm 6.4	78.9 \pm 2.5	76.2 \pm 9.7	74.7 \pm 1.9	69.1 \pm 6.4	73.7 \pm 2.7
	1.5	79.5 \pm 2.6	49.9 \pm 3.7	78.1 \pm 1.2	92.0 \pm 1.7	74.0 \pm 4.5	61.4 \pm 7.4	73.8 \pm 1.1

1091
 1092 Table 6: Performance on ALFWorld and WebShop. Results are averaged over 3 random seeds. For
 1093 ALFWorld, we report the average success rate (%) for each subtask as well as the overall result. For
 1094 WebShop, we report both the average score and the average success rate (%).

Method	ALFWorld							WebShop	
	Pick	Look	Clean	Heat	Cool	Pick2	All	Score	Succ.
<i>Base: LLaMA3.1-8B-Instruct</i>									
RL Training GRPO	92.2 \pm 1.7	63.5 \pm 9.5	79.5 \pm 4.7	86.9 \pm 2.0	68.0 \pm 3.3	78.5 \pm 2.8	79.6 \pm 1.7	85.2 \pm 1.4	68.0 \pm 1.0
with EMPG	96.8 \pm 1.7	81.2 \pm 3.7	93.3 \pm 1.9	82.6 \pm 3.7	79.5 \pm 3.2	82.9 \pm 2.4	87.5 \pm 1.3	86.3 \pm 1.2	70.1 \pm 1.5
<i>Base: Qwen2.5-7B-Instruct</i>									
RL Training GRPO	88.8 \pm 5.6	43.7 \pm 8.2	88.1 \pm 3.5	70.3 \pm 6.9	77.7 \pm 2.3	56.8 \pm 9.4	74.8 \pm 3.1	77.8 \pm 1.4	65.6 \pm 1.0
with EMPG	92.9 \pm 2.9	75.2 \pm 3.8	74.8 \pm 3.9	86.3 \pm 4.7	73.7 \pm 2.6	65.3 \pm 5.8	78.5 \pm 1.7	81.0 \pm 1.4	69.3 \pm 1.5

1103
 1104
 1105
 1106
 1107
 1108
 1109
 1110
 1111
 1112
 1113
 1114
 1115
 1116
 1117
 1118
 1119
 1120
 1121
 1122
 1123
 1124
 1125
 1126
 1127
 1128
 1129
 1130
 1131
 1132
 1133
 1134
 1135
 1136
 1137
 1138
 1139
 1140
 1141
 1142
 1143
 1144
 1145
 1146
 1147
 1148
 1149
 1150
 1151
 1152
 1153
 1154
 1155
 1156
 1157
 1158
 1159
 1160
 1161
 1162
 1163
 1164
 1165
 1166
 1167
 1168
 1169
 1170
 1171
 1172
 1173
 1174
 1175
 1176
 1177
 1178
 1179
 1180
 1181
 1182
 1183
 1184
 1185
 1186
 1187
 1188
 1189
 1190
 1191
 1192
 1193
 1194
 1195
 1196
 1197
 1198
 1199
 1200
 1201
 1202
 1203
 1204
 1205
 1206
 1207
 1208
 1209
 1210
 1211
 1212
 1213
 1214
 1215
 1216
 1217
 1218
 1219
 1220
 1221
 1222
 1223
 1224
 1225
 1226
 1227
 1228
 1229
 1230
 1231
 1232
 1233
 1234
 1235
 1236
 1237
 1238
 1239
 1240
 1241
 1242
 1243
 1244
 1245
 1246
 1247
 1248
 1249
 1250
 1251
 1252
 1253
 1254
 1255
 1256
 1257
 1258
 1259
 1260
 1261
 1262
 1263
 1264
 1265
 1266
 1267
 1268
 1269
 1270
 1271
 1272
 1273
 1274
 1275
 1276
 1277
 1278
 1279
 1280
 1281
 1282
 1283
 1284
 1285
 1286
 1287
 1288
 1289
 1290
 1291
 1292
 1293
 1294
 1295
 1296
 1297
 1298
 1299
 1300
 1301
 1302
 1303
 1304
 1305
 1306
 1307
 1308
 1309
 1310
 1311
 1312
 1313
 1314
 1315
 1316
 1317
 1318
 1319
 1320
 1321
 1322
 1323
 1324
 1325
 1326
 1327
 1328
 1329
 1330
 1331
 1332
 1333
 1334
 1335
 1336
 1337
 1338
 1339
 1340
 1341
 1342
 1343
 1344
 1345
 1346
 1347
 1348
 1349
 1350
 1351
 1352
 1353
 1354
 1355
 1356
 1357
 1358
 1359
 1360
 1361
 1362
 1363
 1364
 1365
 1366
 1367
 1368
 1369
 1370
 1371
 1372
 1373
 1374
 1375
 1376
 1377
 1378
 1379
 1380
 1381
 1382
 1383
 1384
 1385
 1386
 1387
 1388
 1389
 1390
 1391
 1392
 1393
 1394
 1395
 1396
 1397
 1398
 1399
 1400
 1401
 1402
 1403
 1404
 1405
 1406
 1407
 1408
 1409
 1410
 1411
 1412
 1413
 1414
 1415
 1416
 1417
 1418
 1419
 1420
 1421
 1422
 1423
 1424
 1425
 1426
 1427
 1428
 1429
 1430
 1431
 1432
 1433
 1434
 1435
 1436
 1437
 1438
 1439
 1440
 1441
 1442
 1443
 1444
 1445
 1446
 1447
 1448
 1449
 1450
 1451
 1452
 1453
 1454
 1455
 1456
 1457
 1458
 1459
 1460
 1461
 1462
 1463
 1464
 1465
 1466
 1467
 1468
 1469
 1470
 1471
 1472
 1473
 1474
 1475
 1476
 1477
 1478
 1479
 1480
 1481
 1482
 1483
 1484
 1485
 1486
 1487
 1488
 1489
 1490
 1491
 1492
 1493
 1494
 1495
 1496
 1497
 1498
 1499
 1500
 1501
 1502
 1503
 1504
 1505
 1506
 1507
 1508
 1509
 1510
 1511
 1512
 1513
 1514
 1515
 1516
 1517
 1518
 1519
 1520
 1521
 1522
 1523
 1524
 1525
 1526
 1527
 1528
 1529
 1530
 1531
 1532
 1533
 1534
 1535
 1536
 1537
 1538
 1539
 1540
 1541
 1542
 1543
 1544
 1545
 1546
 1547
 1548
 1549
 1550
 1551
 1552
 1553
 1554
 1555
 1556
 1557
 1558
 1559
 1560
 1561
 1562
 1563
 1564
 1565
 1566
 1567
 1568
 1569
 1570
 1571
 1572
 1573
 1574
 1575
 1576
 1577
 1578
 1579
 1580
 1581
 1582
 1583
 1584
 1585
 1586
 1587
 1588
 1589
 1590
 1591
 1592
 1593
 1594
 1595
 1596
 1597
 1598
 1599
 1600
 1601
 1602
 1603
 1604
 1605
 1606
 1607
 1608
 1609
 1610
 1611
 1612
 1613
 1614
 1615
 1616
 1617
 1618
 1619
 1620
 1621
 1622
 1623
 1624
 1625
 1626
 1627
 1628
 1629
 1630
 1631
 1632
 1633
 1634
 1635
 1636
 1637
 1638
 1639
 1640
 1641
 1642
 1643
 1644
 1645
 1646
 1647
 1648
 1649
 1650
 1651
 1652
 1653
 1654
 1655
 1656
 1657
 1658
 1659
 1660
 1661
 1662
 1663
 1664
 1665
 1666
 1667
 1668
 1669
 1670
 1671
 1672
 1673
 1674
 1675
 1676
 1677
 1678
 1679
 1680
 1681
 1682
 1683
 1684
 1685
 1686
 1687
 1688
 1689
 1690
 1691
 1692
 1693
 1694
 1695
 1696
 1697
 1698
 1699
 1700
 1701
 1702
 1703
 1704
 1705
 1706
 1707
 1708
 1709
 1710
 1711
 1712
 1713
 1714
 1715
 1716
 1717
 1718
 1719
 1720
 1721
 1722
 1723
 1724
 1725
 1726
 1727
 1728
 1729
 1730
 1731
 1732
 1733
 1734
 1735
 1736
 1737
 1738
 1739
 1740
 1741
 1742
 1743
 1744
 1745
 1746
 1747
 1748
 1749
 1750
 1751
 1752
 1753
 1754
 1755
 1756
 1757
 1758
 1759
 1760
 1761
 1762
 1763
 1764
 1765
 1766
 1767
 1768
 1769
 1770
 1771
 1772
 1773
 1774
 1775
 1776
 1777
 1778
 1779
 1780
 1781
 1782
 1783
 1784
 1785
 1786
 1787
 1788
 1789
 1790
 1791
 1792
 1793
 1794
 1795
 1796
 1797
 1798
 1799
 1800
 1801
 1802
 1803
 1804
 1805
 1806
 1807
 1808
 1809
 1810
 1811
 1812
 1813
 1814
 1815
 1816
 1817
 1818
 1819
 1820
 1821
 1822
 1823
 1824
 1825
 1826
 1827
 1828
 1829
 1830
 1831
 1832
 1833
 1834
 1835
 1836
 1837
 1838
 1839
 1840
 1841
 1842
 1843
 1844
 1845
 1846
 1847
 1848
 1849
 1850
 1851
 1852
 1853
 1854
 1855
 1856
 1857
 1858
 1859
 1860
 1861
 1862
 1863
 1864
 1865
 1866
 1867
 1868
 1869
 1870
 1871
 1872
 1873
 1874
 1875
 1876
 1877
 1878
 1879
 1880
 1881
 1882
 1883
 1884
 1885
 1886
 1887
 1888
 1889
 1890
 1891
 1892
 1893
 1894
 1895
 1896
 1897
 1898
 1899
 1900
 1901
 1902
 1903
 1904
 1905
 1906
 1907
 1908
 1909
 1910
 1911
 1912
 1913
 1914
 1915
 1916
 1917
 1918
 1919
 1920
 1921
 1922
 1923
 1924
 1925
 1926
 1927
 1928
 1929
 1930
 1931
 1932
 1933
 1934
 1935
 1936
 1937
 1938
 1939
 1940
 1941
 1942
 1943
 1944
 1945
 1946
 1947
 1948
 1949
 1950
 1951
 1952
 1953
 1954
 1955
 1956
 1957
 1958
 1959
 1960
 1961
 1962
 1963
 1964
 1965
 1966
 1967
 1968
 1969
 1970
 1971
 1972
 1973
 1974
 1975
 1976
 1977
 1978
 1979
 1980
 1981
 1982
 1983
 1984
 1985
 1986
 1987
 1988
 1989
 1990
 1991
 1992
 1993
 1994
 1995
 1996
 1997
 1998
 1999
 2000
 2001
 2002
 2003
 2004
 2005
 2006
 2007
 2008
 2009
 2010
 2011
 2012
 2013
 2014
 2015
 2016
 2017
 2018
 2019
 2020
 2021
 2022
 2023
 2024
 2025
 2026
 2027
 2028
 2029
 2030
 2031
 2032
 2033
 2034
 2035
 2036
 2037
 2038
 2039
 2040
 2041
 2042
 2043
 2044
 2045
 2046
 2047
 2048
 2049
 2050
 2051
 2052
 2053
 2054
 2055
 2056
 2057
 2058
 2059
 2060
 2061
 2062
 2063
 2064
 2065
 2066
 2067
 2068
 2069
 2070
 2071
 2072
 2073
 2074
 2075
 2076
 2077
 2078
 2079
 2080
 2081
 2082
 2083
 2084
 2085
 2086
 2087
 2088
 2089
 2090
 2091
 2092
 2093
 2094
 2095
 2096
 2097
 2098
 2099
 2100
 2101
 2102
 2103
 2104
 2105
 2106
 2107
 2108
 2109
 2110
 2111
 2112
 2113
 2114
 2115
 2116
 2117
 2118
 2119
 2

1134
1135**Algorithm 2** Part 1: PyTorch-Style Pseudocode for EMPG Advantage Calculation

```

1 import numpy as np
2 import torch
3
4 def compute_empg_advantage(tokenizer, batch, k=1.0, k_f=1.0, zeta=0.1):
5     """
6     Args:
7         tokenizer: The tokenizer for identifying response segments.
8         batch: A data batch with 'responses', 'old_entropy', 'advantages'
9         .
10        k (float): Hyperparameter for self-calibrating gradient scaling.
11        k_f (float): Hyperparameter for the future clarity bonus.
12        zeta (float): Hyperparameter for the future clarity bonus.
13    """
14    # --- 1. First Pass: Collect Step-Level Entropies ---
15    all_step_entropies = []
16    # segments_to_modify stores {'sample_idx', 'start', 'end'} for each
17    # step
18    segments_to_modify = []
19
20    for i in range(batch.batch.batch_size[0]):
21        # Find "assistant" segments, which correspond to agent steps.
22        token_segments = process_token_sequences(
23            batch.batch['responses'][i],
24            tokenizer.encode("<|im_start|>assistant\n"),
25            tokenizer.encode('<|im_end|>')
26        )
27        for start, end in token_segments:
28            if start >= end: continue
29
30            # Calculate the average token-level entropy for the step
31            step_entropy = batch.batch['old_entropy'][i][start:end].mean
32            .item()
33            all_step_entropies.append(step_entropy)
34            segments_to_modify.append({'sample_idx': i, 'start': start,
35            'end': end})
36
37    if not all_step_entropies: return
38
39
40
41
42
43
44
45
46
47
48
49
50
51
52
53
54
55
56
57
58
59
60
61
62
63
64
65
66
67
68
69
70
71
72
73
74
75
76
77
78
79
80
81
82
83
84
85
86
87
88
89
90
91
92
93
94
95
96
97
98
99
100
101
102
103
104
105
106
107
108
109
110
111
112
113
114
115
116
117
118
119
120
121
122
123
124
125
126
127
128
129
130
131
132
133
134
135
136
137
138
139
140
141
142
143
144
145
146
147
148
149
150
151
152
153
154
155
156
157
158
159
160
161
162
163
164
165
166
167
168
169
170
171
172
173
174
175
176
177
178
179
180
181
182
183
184
185
186
187

```

2. **Modulation Component Calculation:** All collected step entropies $\{H_t\}$ are normalized across the batch using min-max scaling to produce $\{H_{\text{norm},t}\}$ (as per Eq. 8). These normalized values are then used to compute the two key components of our method: the self-calibrating scaling factor $g(H_t)$ (Eq. 6) and the future clarity bonus term $g'(H_{t+1})$ (Eq. 7).
3. **Advantage Modulation:** The function then applies these components to the original outcome-based advantage. For each step, the advantage is scaled by $g(H_t)$ and augmented by the future clarity bonus $\zeta \cdot g'(H_{t+1})$, yielding the modulated advantage A_{mod} as defined in our main formula (Eq. 4).
4. **Final Normalization:** Finally, to reduce variance and ensure stable training, the entire batch of resulting modulated advantages is normalized to have a mean of zero. This produces the final advantage A_{final} (Eq. 9) that is used to compute the policy gradient.

1188

1189

1190

1191

1192

1193

1194

1195

1196

1197

Algorithm 3 Part 2: PyTorch-Style Pseudocode for EMPG Advantage Calculation (cont.)

```

1      # --- 2. Calculate Modulated Advantage Components ---
2      H = np.array(all_step_entropies)
3
4      # Batch-level entropy normalization (Eq. 12) with \epsilon = 1e-8
5      min_H, max_H = np.min(H), np.max(H)
6      H_norm = (H - min_H) / (max_H - min_H + 1e-8)
7
8      # Self-calibrating gradient scaling g(H) (Eq. 10)
9      g_H_unnormalized = np.exp(-k * H_norm)
10     mean_g_H = np.mean(g_H_unnormalized)
11     g_H = g_H_unnormalized / (mean_g_H + 1e-8)
12
13    # Future clarity bonus f(H) (Eq. 11)
14    f_H = np.exp(-k_f * H_norm)
15
16    # Convert to tensors for PyTorch operations
17    g_H = torch.tensor(g_H, device=batch.batch['advantages'].device,
18                        dtype=torch.float32)
19    f_H = torch.tensor(f_H, device=batch.batch['advantages'].device,
20                        dtype=torch.float32)
21
22    # --- 3. Second Pass: Apply Advantage Modulation (Eq. 8) ---
23    step_advantages = []
24    for i, segment in enumerate(segments_to_modify):
25        idx, start, end = segment['sample_idx'], segment['start'],
26        segment['end']
27
28        # Apply self-calibrating gradient scaling
29        batch.batch['advantages'][idx][start:end] *= g_H[i]
30
31        # Add future clarity bonus if there is a next step
32        next_seg = segments_to_modify[i+1] if i+1 < len(
33        segments_to_modify) else None
34        if next_seg and next_seg['sample_idx'] == idx:
35            batch.batch['advantages'][idx][start:end] += zeta * f_H[i+1]
36        step_advantages.append(batch.batch['advantages'][idx][start])
37
38    # --- 4. Final Advantage Normalization (Eq. 7) ---
39    if step_advantages:
40        final_adv_mean = torch.mean(torch.stack(step_advantages))
41        batch.batch['advantages'] -= final_adv_mean

```

1233

1234

1235

1236

1237

1238

1239

1240

1241